Fibers and Polymers 2014, Vol.15, No.9, 1810-1821 DOI 10.1007/s12221-014-1810-7

Modified Polyamide 66 Fibers for the Removal of Reactive Dyes from Aqueous Suspension

Mahjoub Jabli, Mohamed Hamdaoui[1], Ragoubi Marwa, Adnen Haj Ayed, and Béchir Ben Hassine*

Laboratory of Organic, Asymmetric and Homogenous Catalysis, FSM, University of Monastir, Tunisia
[1]Laboratory of Studies of Thermal and Energetic Systems (LESTE), ENIM, University of Monastir, Tunisia
(Received July 4, 2013; Revised October 17, 2013; Accepted December 20, 2013)

Abstract: In this paper, we report the modification of polyamide sample (PA) with different contents of chitosan (CS) using citric acid (CA) as a cross-linker [PA-CA-CS]. New materials were confirmed to be formed in PA using FT-IR spectrum. It is also checked in terms of the change in thermal stability event and decomposition behavior in thermogravimetry through TG-DTA instruments. Then, the ability of unmodified and modified supports was tested for the adsorption of two reactive dyes i.e. Cibacron Brilliant Yellow 3G-P and Cibacron Blue P-3R. Sorption experiments were performed under varying several experimental conditions such as pH, contact time, initial dye concentration, and temperature. The isotherm and kinetic models were undertaken to assess the dye removal mechanism. The applicability of Langmuir, Freundlich, Dubinin-Radushkevich, and Temkin equations was checked and data were fitted using Langmuir model. The second-order equation was shown to fit the adsorption kinetics. Data gleaned from both thermodynamic results and modeling data indicate that the adsorption follows a chemical and exothermic process.

Keywords: Polyamide, Chitosan, Citric acid, Cibacron Brilliant Yellow 3G-P, Cibacron Blue P-3R, Dyeing kinetics, Thermodynamics

Introduction

Adsorption process in the presence of different bio-sorbent materials has been reported in the literature [1]. In particular, chitosan has proved to be an effective bio-sorbent for removing the dyes from aqueous solutions because of its unique characteristics and high sorption capacities [2-5]. In this area, Wan Ngah, *et al*. [6] have reviewed in details the capacity of chitosan composite for the removal of pollutants. The results proved that chitosan is very suitable adsorbent material for a wide range of contaminants, when used alone or in combination with other materials. In our previous contributions, we had reported the synthesis and characterization of a new ternary complex [dye molecules/Cu(II)-glutaraldehyde-chitosan] [7] and we had observed that the use of the macroporous Glut-chitosan microspheres in binding either metal ions and/or ligands is worthy of exploration in the context of the synthesis of ternary complexes. In addition, our data gleaned from chitosan microspheres supported that either [bis(2-methylallyl) (1,5-cyclooctadienne) ruthenium (II)] or ruthenium ions exhibited an excellent ability to degrade dyes in the presence of an ecological oxidant [8]. More importantly, to extend applications, several approaches have shed the light on the blending of chitosan with other natural or synthetic polymers [9-15]. For example, Kim and Min [15] have developed a composite fiber of polyacrylonitrile (PAN) and chitosan by spinning polymer mixture and the obtained composite showed a much higher amount of uptake for acid dye than that of either powdery chitosan or activated carbon. In other example, chitosan is blended with nylon 6 by combining solvent evaporation and a phase inversion technique, where silver ions are chelated to the membranes, and then antibacterial properties were investigated [16]. In other works, nylon fibers were grafted with methacrylic acid (MAA) and the modified samples were used to remove copper (II) ions and dyes from aqueous solutions [17]. Tseng has also reported the grafting of chitosan oligomer or polymer on nylon fabrics after being activated by open air plasma and then checked for antimicrobial experiments [18]. In this area, we have developed [chitosan-cotton] composite materials for acid dye removal from aqueous suspension using an easy and economical technique [19]. Our other previous experiments had also focused on the synthesis and the examination of the complex [Cu(II)/cellulose-chitosan] for immobilizing Calmagite, Acid Blue 25, and Erio Black B as dye ligands in batch system [20].

A number of competent systems based on the chemical modification of natural substrates or synthetic polymer have been particularly investigated for the treatment of effluents. Attention has been, continuously, focused on the development of effective and low cost adsorbents. The purpose of the present study was to improve dye removal from aqueous solution by adsorption using functionalized polyamide fibers. So, we conduct our research for the modification of polyamide fibers with different content of chitosan in the presence of either citric acid or acetic acid. Unmodified and prepared materials were characterized using FT-IR and TGA-DTA instruments. Then, their capabilities for the removal of Cibacron Brilliant Yellow 3G-P and Cibacron Blue P-3R from aqueous suspension were studied and compared in terms of pH, contact time, temperature, and initial dye concentration. The equilibrium data were analyzed using

*Corresponding author: bechirbenhassine@yahoo.fr

Langmuir, Freundlich, Temkin, and Dubinin-Radushkevich isotherm models. Kinetic equations were also applied and the associated parameters were deduced. Thermodynamic constants were determined in order to define the nature of the adsorption process of the studied dyes on the surface of each prepared material.

Experimental

Materials and Reagents

The polyamide 66 (PA 66) sample was supplied by SITEX (International Society of Textile, Sousse, Tunisia). To remove impurities, PA was subjected to a treatment bath with a liquor ratio of 1:50 (w/v) containing a non-ionic detergent (2 %) for 2 h, at a temperature of 60 °C. Chitosan (CS) from crab shell was purchased from Sigma Aldrich (Sigma-Aldrich Chimie Sarl, Saint-Quentin Fallavier, France) as a powder with a deacetylation degree of 72.50 and was used without further purification. Cibacron Brilliant Yellow 3G-P [$C_{25}H_{15}C_{l3}N_9\ Na_3\ O_{10}S_3$, M.W = 872.96 g·mol^{-1}, referred to as CBY] and Cibacron Blue P-3R [$C_{32}H_{23}ClN_7Na_3O_{11}S_3$, M.W=882.18 g·mol^{-1}, referred to as CBP] were supplied by Hoechst (Frankfort, Germany) in the form of sodium salts. Their chemical structures were depicted in Figure 1. The stock dye solutions were prepared by dissolving appropriate amount of CBY and CBP in 500 m*l* of distilled water. The working solutions were obtained by diluting the dye stock solutions to the required concentrations. Analytical grade HCl and NaOH were obtained from Merck. Distilled water was used to prepare all solutions.

Modification of PA Samples

The PA modification procedure was similar to procedures adopted in our previous work [19] and described by Hsieh *et al.* [21]. CS solution was prepared by stirring a weighed amount of CS powder (0.05, 0.1, 0.25, and 0.5 g) in 1 % (v/v) aqueous acetic acid solution or in 10 % (w/v) citric acid until complete dissolution at room temperature. After that, PA samples were immersed directly in 100 m*l* aqueous solutions of CS, squeezed to a wet pick up of 100 %, pinned to the original dimensions, and dried at 120 °C for 2 min. Further, samples were thoroughly rinsed with distilled water to remove the non-reacted amount of CS, rinsed with hot and cold water and finally oven-dried. Four samples of modified PA, with different weight add-on, were obtained. The weight add-on was defined according to the equation:

$$\text{Weight add-on} = \frac{M_f - M_0}{M_0} \times 100 \quad (1)$$

where M_0 and M_f are the initial mass of PA sample before and after modification, respectively.

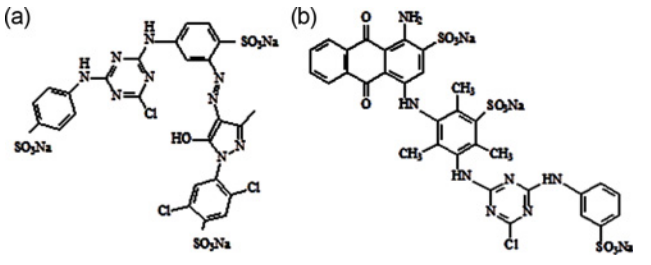

Figure 1. Chemical structure of (a) Cibacron Brilliant Yellow 3G-P and (b) Cibacron Blue P-3R.

Characterization of Unmodified and Modified PA Samples

FT-IR Spectrum

The FT-IR spectra were obtained from potassium bromide (KBr) pellets using a FT-IR spectrometer (Perkin-Elmer FT-IR System 2000 Model spectrometer, CRBJ, Borj Cidria, Tunisia) operating in a transmission mode with a resolution of 2 cm^{-1} in the range of 400-4000 cm^{-1}. Dry globules of unmodified and modified PA were crushed and ground in a mortar by pestle, and then the fine powder was mixed with KBr, pressed into a thin pellet, and placed in the sample holder of the spectrometer.

Thermal Analysis (TGA and DTA)

For the differential thermal analysis (DTA) and for the thermogravimetric analysis (TGA), approximately 8-10 mg of each material in an alumina crucible was heated from 40 to 800 °C at a heating rate of 10 °C/min under an air atmosphere. The mass of the sample was recorded as a function of temperature. The DTA and TGA curves were obtained, using a TA Instruments SDT-2960 device (ISET, Ksar Hellal, Tunisia).

Adsorption and Kinetic Experiments

The adsorption process of unmodified and modified PA samples [PA, PA-CA-CS: (0.05-0.5 %)] was performed using a batch method. Flasks were maintained at 22.0±0.5 °C containing a weighted corresponding adsorbent (0.5 g) and 100 m*l* of the dye solution (CBY or CBP) in a wide range of concentrations (from 5 to 500 mg/*l*). The system was continuously stirred at 150 rpm until the equilibrium was reached. For pH effect studies, the adsorption of CBY and CBP was tested in pH range 2-12, through adjusting it using either HCl or NaOH (0.10 M). The adsorbents were then separated from the solution and the concentration of dye in each solution was determined by absorbance measurements using a calibration curve at maximum wavelength (λ_{max}= 403 nm for CBY and λ_{max}=588 nm for CBP). For kinetic experiment studies, each adsorbent was thoroughly mixed individually with 50 m*l* of dye solutions (50 and 100 mg/*l*) and the suspensions were conducted at room temperature. Samples of 1.0 m*l* were collected from the duplicate flasks at required time intervals and the absorbance value was registered.

Results and Discussion

Characterization of Unmodified and Modified PA Samples

Determination of CS Content on Modified PA Samples

Figure 2 represents the evolution of the weight add-on as a

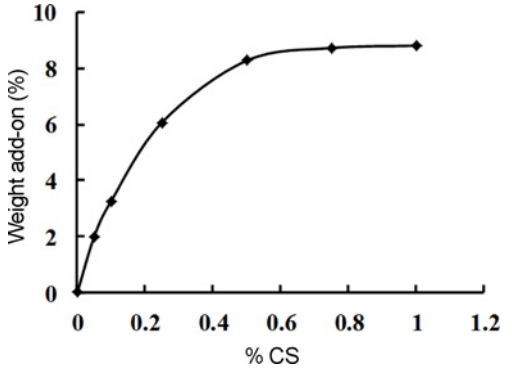

Figure 2. Evolution of the weight add-on as a function of CS content in bath treatment.

function of CS concentration in bath treatment. Data reveals that the weight add-on after the application of CS to PA sample is slightly higher and it increases with the increment in the concentration of CS in the bath treatment. This could be related to the viscosity and solubility properties of this polymer. It has been observed that when achieving a value of 0.5 %, the weight add-on becomes constant and this behavior could be explained by the fact that below this value, reactive sites of PA are available to react with functional groups of CS after which there is no accessibility. The high viscosity of large concentrations of CS could also prevent the diffusion of the solution into the PA fibers.

FT-IR Analysis

The characteristic bands for PA were observed at 3404 cm^{-1} (N-H stretch vibration), 1564 cm^{-1} (amide I, CO stretch), and 1514 cm^{-1} (amide II, CO-N-H band) ((Figure 3(a)) [22]. Spectrum of pure CS shows peaks at around 1610 and 1366 cm^{-1} ((Figure 3(b)), which are characteristic of chitin and chitosan and reported as amide I and III, respectively [23,24]. The peak at 1440 cm^{-1} was assigned to the CH_3 symmetrical deformation mode. The peak at 1090 cm^{-1} indicates the C-O stretching vibration. Peak at 3024 cm^{-1} is the typical C-H stretch vibration. The broad absorption band in the range of 3510 cm^{-1} is attributed to N-H and OH stretching vibrations and intermolecular hydrogen bonding of the polysaccharide molecules. Comparing the IR spectrum of unmodified ((Figure 3(a)) and modified PA samples ((Figure 3(c-f)), we observe a strong characteristic stretching vibration absorption band of carboxyl group at 1732 cm^{-1} in IR spectrum of citric acid modified PA samples. Such a result confirms the citric acid esterification. In addition, the broad absorption OH shifts to higher frequency from about 3404 for PA to 3506 cm^{-1} for PA-CA-CS: 0.25 % ((Figure 3(c-f)) confirming the existence of more O-H groups after citric acid modification. Our finding data were in agreement with the works of Hsieh *et al.* [21], when studying the treatment of wool fabric with citric acid and chitosan.

TGA-DTA Analysis

Additional evidence of the chemical modification of PA

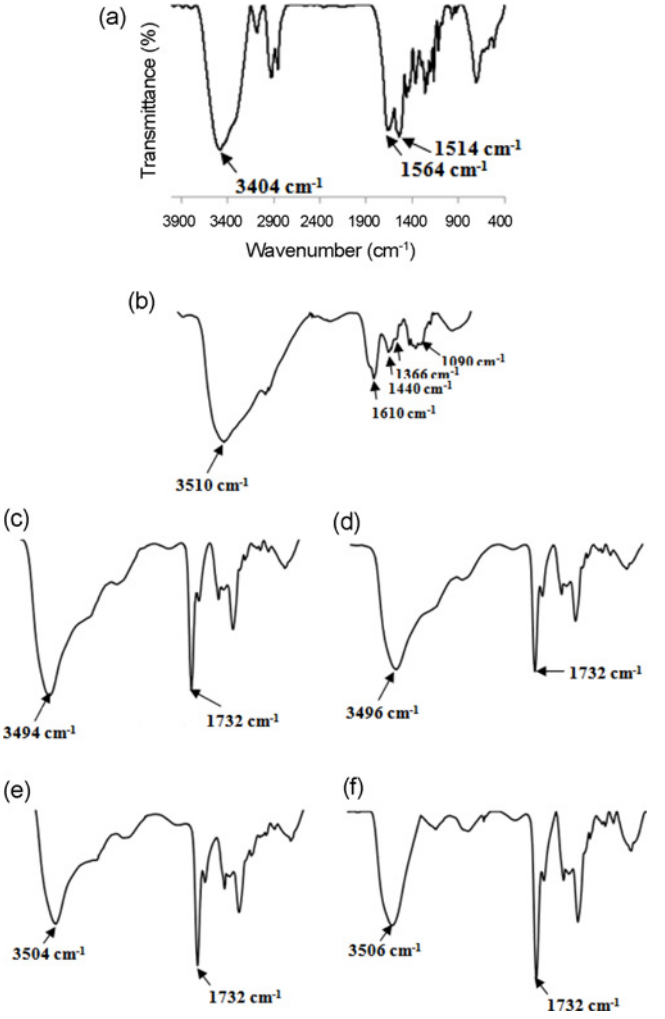

Figure 3. FT-IR spectrum of (a) PA, (b) CS, (c) PA-CA-CS (0.05 %), (d) PA-CA-CS (0.1 %), (e) PA-CA-CS (0.25 %), and (f) PA-CA-CS (0.5 %).

fibers was also confirmed from the change in thermal stability event and in the decomposition behavior in thermogravimetry analysis. Figures 4-8 illustrate the dynamic TGA and DTA curves of unmodified PA and different prepared PA-CA-CS materials. Results display an endothermic peak at about 56 °C, connected with 3 % mass loss, and it was attributed to the evaporation of water absorbed in the inner polymer [25]. The loss of mass in this temperature range is practically identical for all samples indicating an insignificant change in moisture regain. A series of other endothermic peaks were also observed at 226, 438, and 460 °C (Figure 4) and could correspond to the evaporation of some volatile compounds after polymer decomposition. The observed strong exothermic peaks at 558 °C (Figure 4), 555 °C (Figure 5), 557 °C (Figure 6), 575 °C (Figure 7), and 561 °C (Figure 8) are due to the oxidative decomposition of the charred residues of the unmodified and modified polymer [25]. The exothermic peak is also interrupted by a strong endotherm peak at 475 °C and it may correspond to

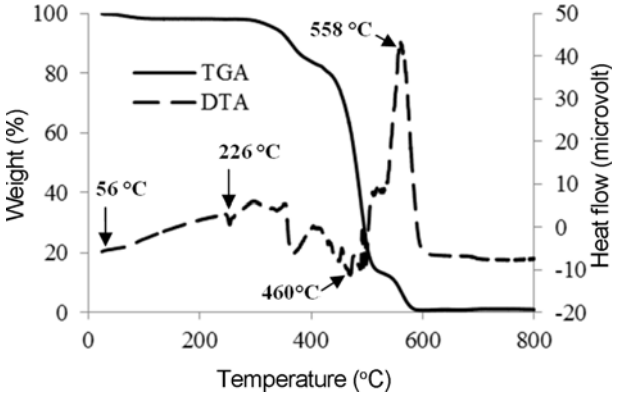

Figure 4. TGA and DTA curves of PA (10 °C/min in the presence of O_2).

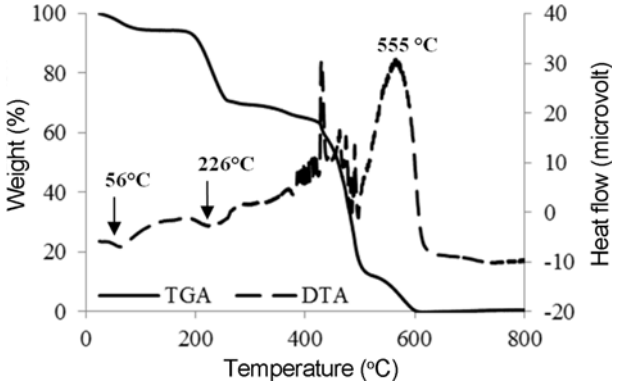

Figure 5. TGA and DTA curves of PA-CA-CS (0.05 % in the presence of O_2).

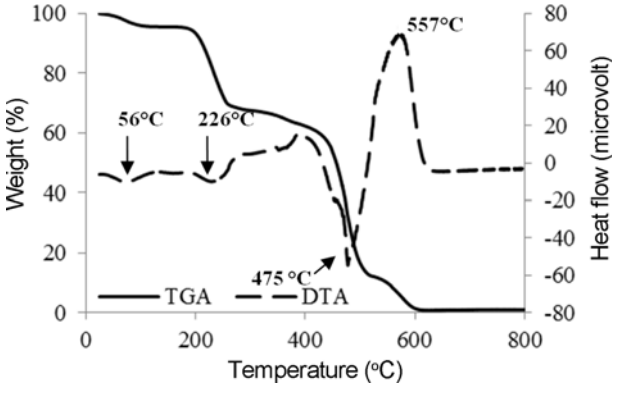

Figure 6. TGA and DTA curves of PA-CA-CS (0.1 % in the presence of O_2).

the scission of the incorporated ester groups from the compound (modified polymer). This peak was not observed in the spectrum of PA. The change in the value of the temperature of oxidation from 558 to 575 °C could be explained by the presence of citric acid which reacts as a cross-linked agent between PA and CS molecules. Such event could again confirm the formation of the novel compounds.

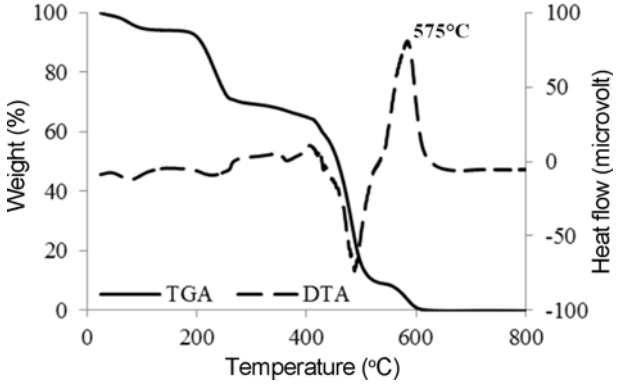

Figure 7. TGA and DTA curves of PA-CA-CS (0.25 % in the presence of O_2).

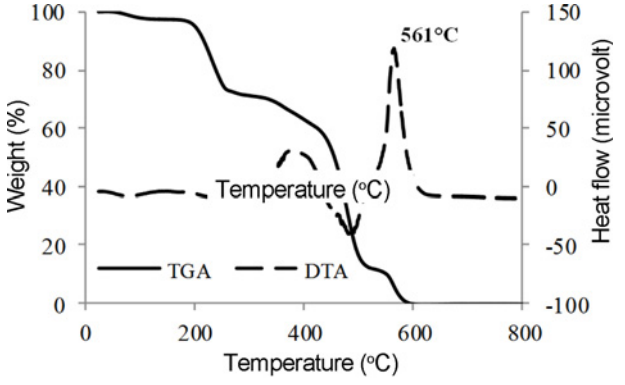

Figure 8. TGA and DTA curves of PA-CA-CS (0.5 % in the presence of O_2).

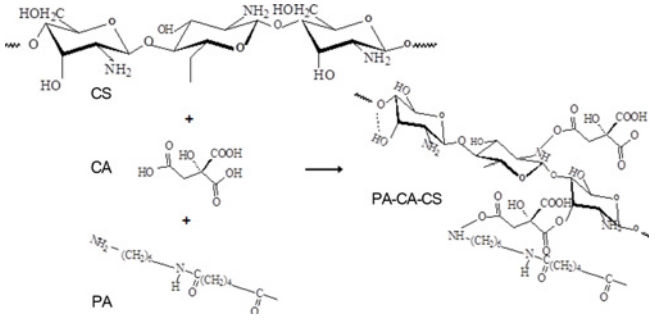

Figure 9. A sort of interaction between CA, PA, and CS molecules.

Based on FT-IR and TGA-DTA analysis, a sort of interaction between CA, CS, and PA was proposed (Figure 9). Indeed CA, as a trivalent acid, could bind PA and CS molecules via the presence of both amino and hydroxyl groups.

Effect of Experimental Parameters on CBY and CBP Adsorption from Aqueous Suspension

Effect of Acid Nature

Figure 10 shows the variation of the adsorbed quantity of

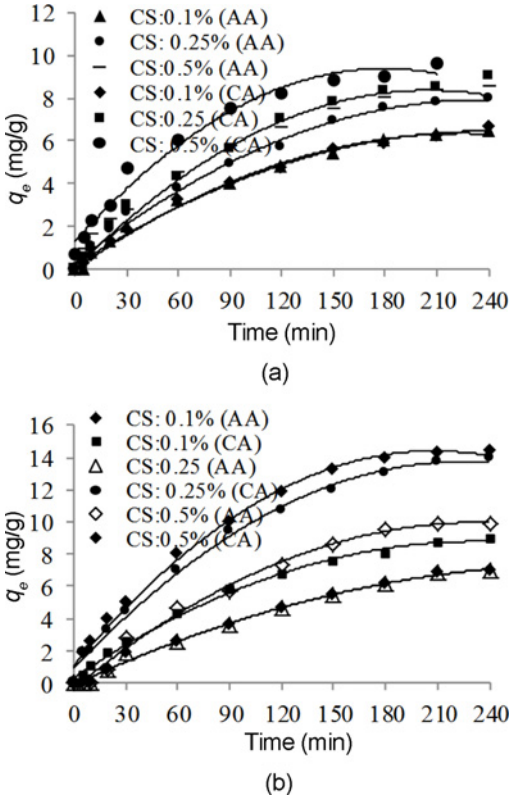

Figure 10. Effect of the variation of acid sort on (a) CBP and (b) CBY removal using modified PA samples.

CBY and CBP on modified PA materials with the nature of the acid. We observe that the adsorption capacity is acid type dependent. As example, when acetic acid is used, the removal of CBY and CBP using [PA-CS: 0.5 %] as adsorbent are, respectively, 9.9 and 8.5 $mg \cdot g^{-1}$. When CA is used, these values reached 14.4 and 10 $mg \cdot g^{-1}$ at the same conditions (mass of adsorbent=0.5 g, time=240 min and T=22 °C). This result explains that CA could play a double role not only to dissolve the CS polymer but also to act as a cross-linking agent. In fact, CS enriched with free hydroxyl and amino groups may bind some carboxyl groups of trivalent acid and therefore an ester linkage could be formed. However, in the case of the monovalent acid (AA), the cross-linking effect could not occur and the interaction between CS and PA is therefore weak.

Effet of pH

The sorption capacity of [PA-CA-CS] was significantly affected by the initial pH value of the aqueous solution. Figure 11 represents the influence of pH value on the removal of both CBY and CBP on [CA-PA-CS] from aqueous solution of an initial concentration of 50 $mg \cdot l^{-1}$. The pH was varied in this experiment between 2 and 12, while keeping all other parameters constant. The sorption capacity (q_e) increases with increasing pH until a value of 3.0 for CBY and 5.0 for CBP (these values were selected for performing

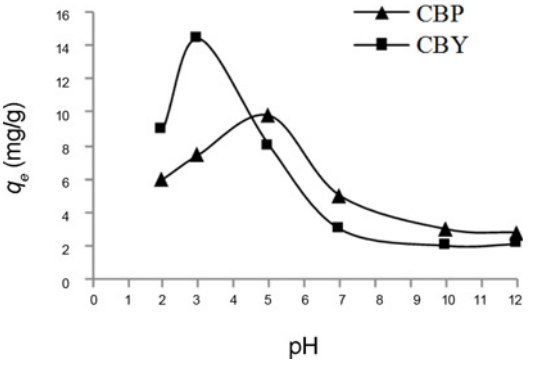

Figure 11. Effect of pH on CBY and CBP removal [experimental conditions: C_0=50 $mg \cdot l^{-1}$, T=22 °C in the presence of PA-CA-CS: 0.5 %].

the subsequent experiments). In fact, at these lower pH values, more protons will be available to protonate some amino groups of CS to form positively charged sorption sites. This increases the electrostatic attraction between negatively charged dye and positively charged sites. However, at pH>7, the adsorption of both dyes decreased dramatically. This could be explained by the fact that at high pH values, more OH^- will be available in the aqueous solution and protonation of amine groups of the adsorbent will not occur.

Effect of Time Contact

Figures 12 and 13 show the time required to reach equilibrium for the adsorption process of either CBY or CBP on the surface of each modified PA material. From the experimental data, we observe that the adsorbed quantity of dye increases with the increase in contact time until a stabilization was reached at high time values (steady state after 120 min and 150 min, respectively, for CBY and CBP). The fast rate achieved from the first minutes can be interpreted based on the fact that in the beginning of the process, more sites are available at the surface of the adsorbent than at equilibrium. As also observed, kinetic data reveals that the materials (PA-CA-CS) fixed more CBY molecules than the CBP. This difference in terms of capacity removal could be probably due to the variance in structure and the molecular weight of the two dyes (Figure 1). More importantly, data showed that the unmodified PA samples exhibited no affinity for the two studied dyes. However, the capacity removal for CBY and CBP increases greatly with the content of CS attached to PA fibers. It ranges, for example, from 1.9 $mg \cdot g^{-1}$ (plain PA) to 28 $mg \cdot g^{-1}$ (PA-CA-CS: 0.5%) for a CBY concentration of 100 $mg \cdot l^{-1}$. This quantity of color adsorbed on modified PA attains nearly its maximum when the concentration of CS in the bath treatment is about 0.5 %. These high sorption capacities prove that the prepared materials could be viewed as efficient competitive adsorbents for color removal.

Effect of Temperature

It is well known that temperature affects the equilibrium

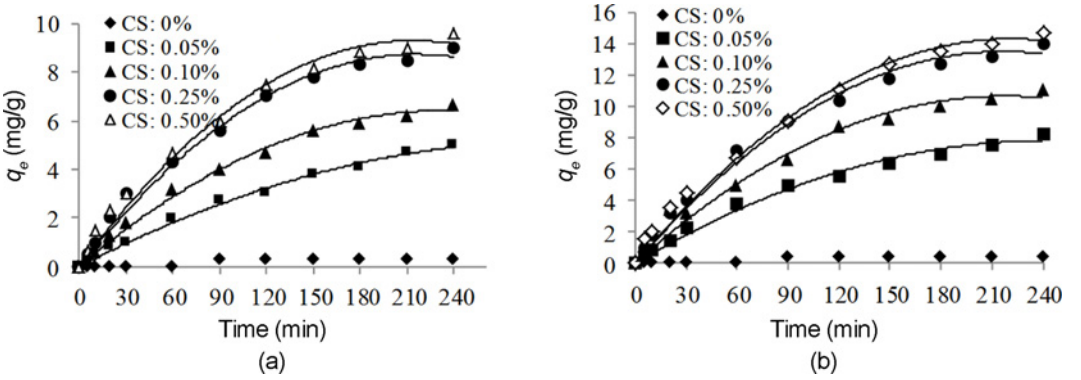

Figure 12. Effect of time contact of CBP removal in the presence of unmodified and modified PA: (a) C_0=50 mg·l^{-1} and (b) C_0=100 mg·l^{-1}.

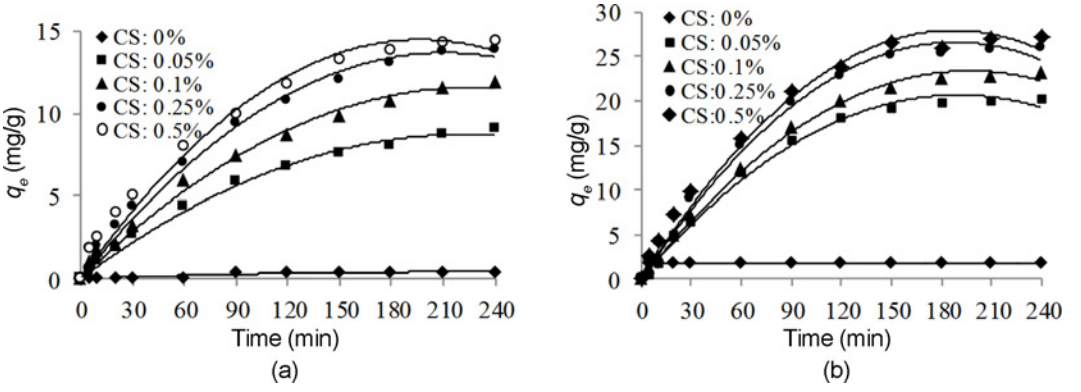

Figure 13. Effect of time contact of CBY removal in the presence of unmodified and modified PA: (a) C_0=50 mg·l^{-1} and (b) C_0=100 mg·l^{-1}.

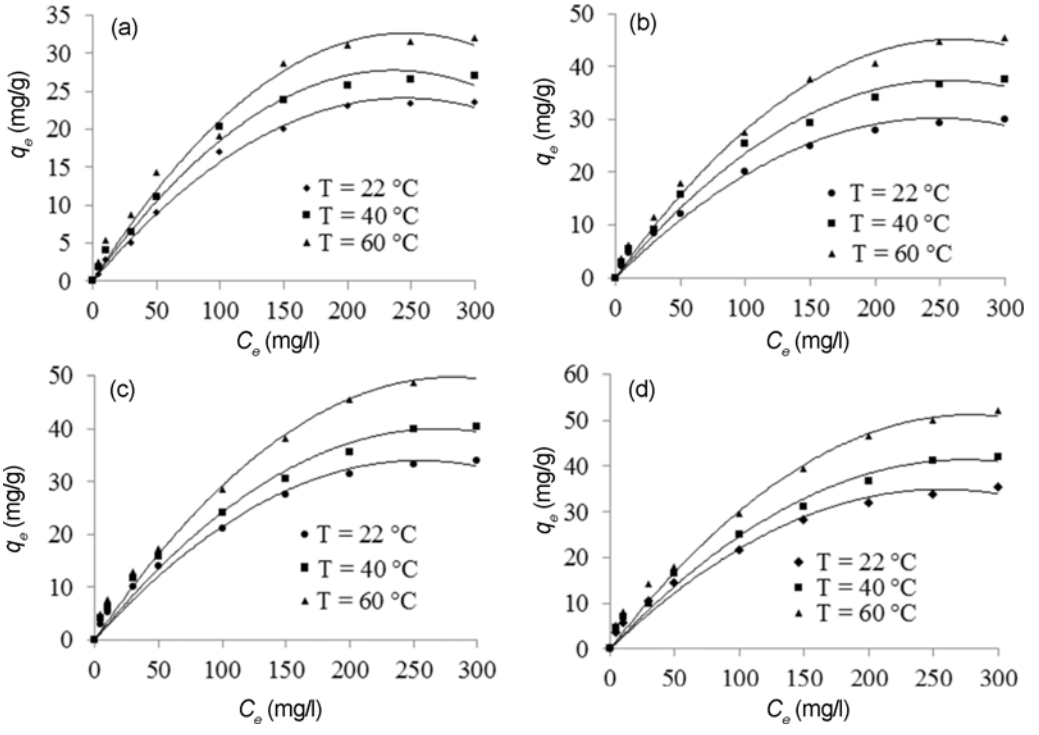

Figure 14. Effect of temperature on the removal of CBY in the presence of different modified PA samples: (a) PA-CA-CS 0.05 %, (b) PA-CA-CS 0.1 %, (c) PA-CA-CS 0.25 %, and (d) PA-CA-CS 0.5 %.

position in relation with the exothermic or the endothermic nature of the process and the swelling capacity of the adsorbent. In these experiments, the effect of the temperature on the adsorption of CBY and CBP on the surface of each modified PA material was studied. For example, in Figure 14, we give the corresponding experimental data related to CBY. As registered, for the two studied dyes CBY and CBP, the adsorption capacity of the adsorbents increases with increasing temperature. This explains the endothermic effect of the adsorption process. As example, the adsorbed quantities of CBY using PA-CA-CS: 0.5 %, as adsorbent, increased from 35.4 $mg \cdot g^{-1}$ at 22 °C to 52 $mg \cdot g^{-1}$ at 60 °C. The higher registered adsorption capacities, compared to room temperature, indicate that the modified PA materials are more efficient as adsorbents at high temperature values.

Kinetic Modeling of the Adsorption of Dyes on the Modified PA Samples

In order to better understand the mechanism of the adsorption of either CBY or CBP on each modified PA sample, the pseudo first-order [26], the pseudo second-order [27], the Elovich [28], and the intra-particle diffusion [29] models

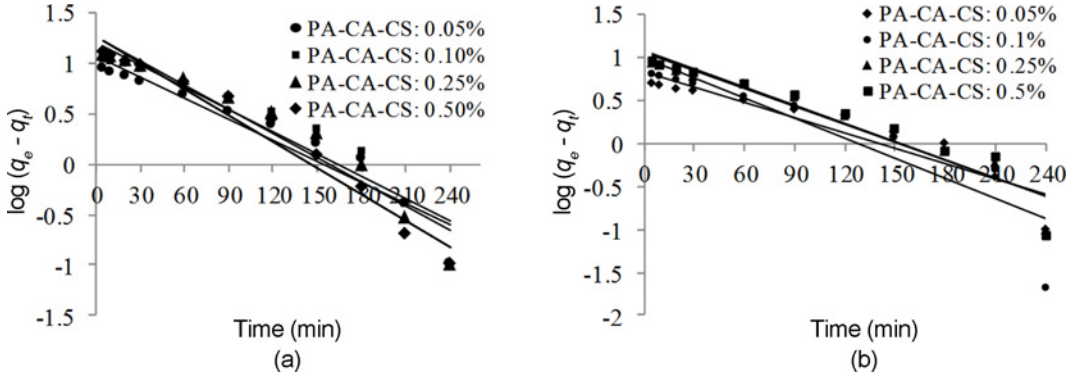

Figure 15. Pseudo first-order kinetic plots for the adsorption of (a) CBY and (b) CBP on the surface of modified PA samples.

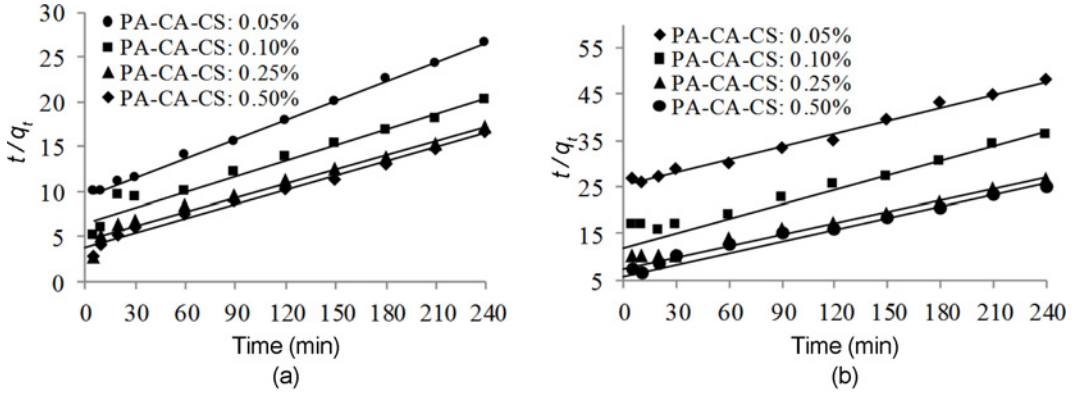

Figure 16. Pseudo second-order kinetic plots for the adsorption of (a) CBY and (b) CBP on the surface of modified PA samples.

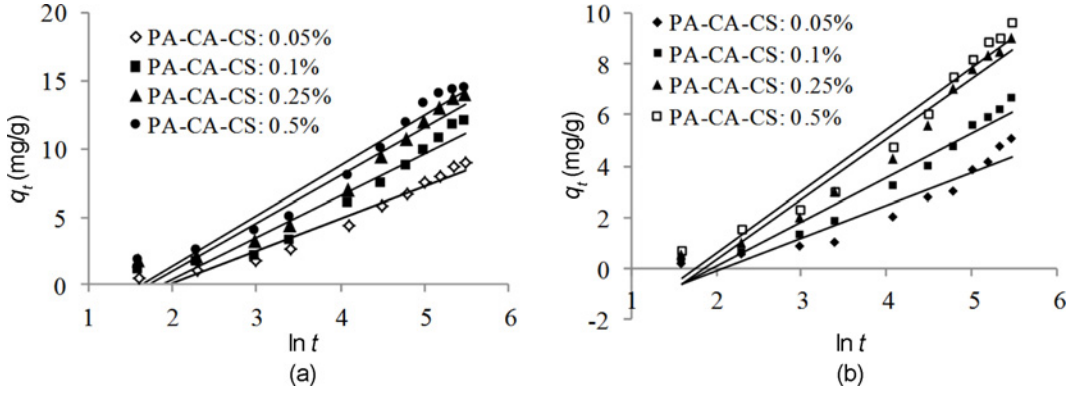

Figure 17. Elovich kinetic plots for the adsorption of (a) CBY and (b) CBP on the surface of modified PA samples.

were used to fit the experimental data. The plots of $\log(q_e-q_t)$ versus time were used to determine the first-order rate constant K_1 (Figure 15). The plots of t/q_t versus time were used to calculate the second-order rate constant K_2 (Figure 16). q_t versus ln t yielded the Elovich constants, a [initial sorption rate ($mg \cdot g^{-1} \cdot min^{-1}$)] and b [extent of surface coverage ($mg \cdot g^{-1} \cdot min^{-1}$)] (Figure 17). While the plots of q versus $t^{1/2}$ yielded the intra-particle diffusion constant, K_i

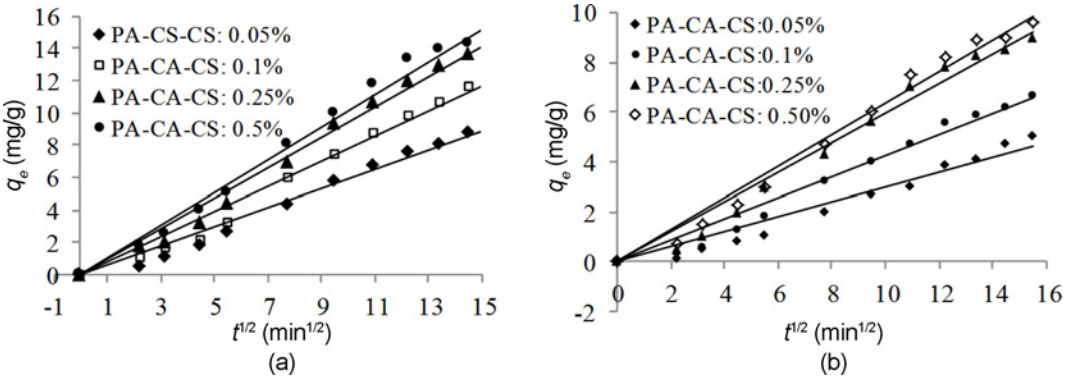

Figure 18. Intra-particle diffusion kinetic plots for the adsorption of (a) CBY and (b) CBP on the surface of modified PA samples.

Table 1. Kinetic constants for the adsorption of CBY on the surface of the surface of modified PA samples

	Pseudo-first order			Pseudo-second order			Elovich			Intra-particle	
$[C_0]$	K_1	q_e	R^2	K_2	q_e	R^2	a	b	R^2	K_i	R^2
0.05 %											
50	0.007	11.67	0.921	0.0000517	14.28	0.998	0.35	0.42	0.955	0.585	0.977
100	0.009	25	0.98	0.000328	30.3	0.987	0.87	0.17	0.972	1.438	0.951
0.1 %											
50	0.007	16.1	0.907	0.000495	17.54	0.958	0.53	0.32	0.939	0.773	0.979
100	0.008	29.44	0.966	0.000222	37.04	0.976	1.29	0.14	0.96	1.616	0.962
0.25 %											
50	0.008	18.49	0.935	0.00062	18.86	0.97	0.65	0.28	0.943	0.936	0.986
100	0.009	32.36	0.983	0.000328	37.04	0.99	1.3	0.14	0.967	1.856	0.968
0.5 %											
50	0.008	18.49	0.968	0.000759	18.87	0.985	0.73	0.27	0.958	1.007	0.985
100	0.009	33.11	0.952	0.000359	37.04	0.99	1.57	0.13	0.966	1.95	0.967

Table 2. Kinetic constants for the adsorption of CBP on the surface of the surface of modified PA samples

	Pseudo-first order			Pseudo-second order			Elovich			Intra-particle	
$[C_0]$	K_1	$q_{e.1}$	R^2	K_2	$q_{e.2}$	R^2	α	β	R^2	K_i	R^2
0.05 %											
50	0.005	6.68	0.881	0.00047	9.43	0.99	0.16	0.78	0.915	0.297	0.952
100	0.006	10.52	0.895	0.000459	13.51	0.991	0.29	0.48	0.947	0.508	0.968
0.1 %											
50	0.007	9.77	0.804	0.000910	9.61	0.97	0.24	0.57	0.952	0.424	0.973
100	0.007	13.64	0.908	0.000827	14.49	0.98	0.50	0.37	0.937	0.724	0.986
0.25 %											
50	0.006	13.64	0.93	0.000952	12.05	0.96	0.37	0.42	0.960	0.593	0.978
100	0.007	18.071	0.887	0.000471	20	0.994	0.56	0.28	0.957	0.915	0.983
0.5 %											
50	0.007	11.93	0.904	0.001183	12.05	0.97	0.39	0.41	0.955	0.634	0.985
100	0.008	20.7	0.864	0.000395	23.25	0.98	0.62	0.27	0.939	0.964	0.985

($mg \cdot g^{-1} \cdot min^{1/2}$) (Figure 18).

The results of rate constant studies for different modified PA samples were summarized in Tables 1 and 2. The assessment of the kinetic models is controlled by the extent of the regression coefficient R^2. In this study, the pseudo second order equation described well the adsorption phenomenon whereas the pseudo first order model fits poorly the experimental data to the whole range of concentrations. The deviation of the straight line from the origin, in the intra-particle diffusion model, may be due to the difference between the rate of mass transfer in the initial and final stages of adsorption [30] (Figure 18).

Analysis of the Adsorption Process of CBY and CBP via Langmuir, Freundlich, Temkin, and Dubinin-Redushkevich Models

In these experiments, the correlation of the amount of adsorption and the liquid-phase concentration was checked via Langmuir [31], Freundlich [32], Temkin [33], and Dubinin-Radushkevich [34] equations (Table 3). Thus, linear regression is frequently used to determine the best-fitting isotherm and the applicability of each model is compared by judging the correlation coefficients. A plot of C_e/q_e versus C_e yields the Langmuir constants q_m and K_L. The plots of ln q_e versus ln C_e were used to calculate the Freundlich parameters such as K_F and n. q_e versus ln C_e yielded the Temkin constants; B_T [related to the heat of adsorption] and A_T [equilibrium binding constant]. While the plots of ln q_e versus ε^2 yielded the Dubinin-Radushkevich constants; the adsorption capacity ($B_{D\text{-}R}$) and the free energy of adsorption (E).

Tables 4 and 5 summarize the parameters values for the different studied dyes/modified PA samples systems. Based on the registered regression coefficients (R^2>0.99), the Langmuir equation strongly supports the fact that the adsorption of studied dyes follows this model. Also seen, in

Table 3. Summary of isotherm equations used for the modeling of dye adsorption on the different modified PA samples

Isotherm	Equation	Linearized form	Plots
Langmuir	$\frac{q_e}{q_m} = \frac{K_L C_e}{1 + K_L C_e}$	$\frac{C_e}{q_e} = \frac{1}{q_{m,L} K_L} + \frac{C_e}{q_{m,L}}$	$\frac{C_e}{q_e} = f(C_e)$
Freundlich	$q_e = K_F + C_e^{(1/n)}$	$\ln q_e = \ln K_F + \left(\frac{1}{n}\right) \ln C_e$	$\ln q_e = f(\ln C_e)$
Temkin	$q_e = B_T \cdot \ln(A_T \cdot C_e)$	$q_e = B_T \ln(A_T) + B_T \ln(C_e)$	$q_e = f(\ln C_e)$
Dubinin-Redushkevich	$q_e = q_{m,DR} \cdot e^{-B\varepsilon^2}$	$\ln(q_e) = \ln((q_{m,DR}) - B\varepsilon^2)$	$\ln q_e = f(\varepsilon^2)$

Table 4. Langmuir, Freundlich, Temkin, and Dubinin-Redushkevich constants for the adsorption of CBY on the surface of modified PA samples

	Langmuir			Freundlich			Temkin			Dubinin-Redushkevich			Parameters		
T (°C)	q_m	K_L	R^2	K_F	n	R^2	B_T	A_T	R^2	$q_{m.DR}$	E	R^2	$\Delta H°$	$\Delta S°$	$\Delta G°$
0.05 %															
22	27.02	0.0181	0.993	1.184	1.818	0.963	5.378	0.238	0.966	15.81	223.607	0.714			9.73
40	31.25	0.0225	0.991	2.604	2.347	0.984	5.547	0.344	0.978	19.41	267.261	0.725	5.543	-14.22	9.99
60	37.04	0.0236	0.990	3.336	2.404	0.980	6.883	0.361	0.979	23.64	288.675	0.724			10.28
0.1 %															
22	29.41	0.0196	0.997	1.523	1.916	0.971	5.866	0.254	0.98	17.85	223.607	0.737			9.611
40	38.46	0.0228	0.992	3.115	2.294	0.969	7.037	0.326	0.982	23.97	250.000	0.763	6.257	-11.37	9.816
60	43.47	0.0267	0.991	4.237	2.457	0.968	8.110	0.404	0.984	29.17	288.675	0.774			10.043
0.25 %															
22	32.25	0.0206	0.995	1.857	1.988	0.969	6.387	0.271	0.977	19.95	223.607	0.745			9.48
40	41.66	0.0245	0.992	3.633	2.375	0.973	7.683	0.363	0.978	26.57	267.261	0.747	7.064	-8.19	9.63
60	50.00	0.0292	0.994	5.501	2.632	0.969	8.832	0.475	0.985	33.18	288.675	0.746			9.79
0.5 %															
22	34.48	0.0215	0.990	2.221	2.075	0.965	6.825	0.282	0.958	21.54	235.702	0.731			9.35
40	43.12	0.0266	0.991	4.072	2.457	0.963	7.780	0.405	0.979	27.94	267.261	0.759	7.766	-5.37	9.45
60	52.63	0.0316	0.995	6.104	2.681	0.963	9.269	0.509	0.980	35.52	288.675	0.743			9.55

Table 5. Langmuir, Freundlich, Temkin, and Dubinin-Redushkevich constants for the adsorption of CBP on the surface of modified PA samples

	Langmuir			Freundlich			Temkin			Dubinin-Redushkevich			Parameters		
T (°C)	q_m	K_L	R^2	K_F	n	R^2	B_T	A_T	R^2	q_{mDR}	E	R^2	ΔH^o	ΔS^o	ΔG^o
							0.05 %								
22	11.9	0.017164	0.997	0.504	1.805	0.965	2.332	0.221	0.981	6.92	223.607	0.757			10.006
40	15.87	0.017346	0.996	0.733	1.862	0.972	3.088	0.235	0.983	9.25	235.702	0.760	0.289	-32,94	10.599
60	20.4	0.017457	0.992	0.952	1.876	0.977	3.985	0.241	0.967	11.66	250.000	0.703			11.258
							0.1 %								
22	18.86	0.01367	0.997	0.596	1,672	0.969	3.602	0.204	0.976	10.08	223.607	0.769			10.534
40	22.72	0.01475	0.992	0.876	1,789	0.984	4.342	0.212	0.966	12.07	235.702	0.760	5.118	-18,36	10.865
60	25.64	0.01764	0.992	1.266	0.919	0.979	4.960	0.242	0.968	14.73	250.000	0.724			11.232
							0.25 %								
22	20.4	0.0197	0.997	0.977	1.537	0.952	4.095	0.257	0.984	12.32	223.607	0.731			9.64
40	23.26	0.0213	0.991	1.678	2.198	0.980	4.419	0.302	0.970	14.27	250.000	0.721	5.338	-14.583	9.90
60	30.3	0.0257	0.996	2.351	2.044	0.958	5.825	0.347	0.987	20.15	267.261	0.808			10.19
							0.5 %								
22	20.83	0.0215	0.995	1.297	2.035	0.938	3.961	0.306	0.987	13.24	223.607	0.831			9.42
40	26.31	0.0236	0.990	2.318	2.318	0.978	4.929	0.352	0.971	16.72	267.261	0.707	5.456	-13.43	9.66
60	31.25	0.0282	0.997	1.723	2.723	0.939	5.873	0.393	0.989	21.22	267.261	0.83			9.93

all cases, the value of $1/n$ were found to be less than 1 indicating that the process was favorable [35]. The Temkin constant, B_T, showed that the heat of adsorption of CBY and CBP on the surface of each studied modified PA sample increased at higher temperatures indicating an endothermic process which is also consistent with the results gleaned from the effect of temperature. In addition, the calculated free energy values ($E_{R\text{-}D}$) from Dubinin-Redushkevich ranged from 223.6 to 288.67 kJ·mol^{-1}. These high values indicate a chemical-sorption [36]. This result is also in agreement with kinetic data described by the second order model, as mentioned previously. In the works of Ikhlass [37], high values of $E_{R\text{-}D}$ (between 50 and 112 kJ·mol^{-1}) were registered for the removal of removal of chromium (VI) using activated alumina and donnan dialysis. Selvaraj Rengaraj *et al.* [38] found elevated values (between 3535.5 and 5972.94 kJ·mol^{-1}) when studying the adsorption characteristics of Cu(II) onto ion exchange resins 252H and 1500H.

Thermodynamics of the Adsorption of CBY and CBP on the Surface of Modified PA Samples

The standard Gibbs free energy change (ΔG^o) for the adsorption process can be calculated using the following equation [39]:

$$\Delta G^o = -RT\ln K_L \quad (1)$$

where R is the gas constant (8.314 J·mol^{-1}·K^{-1}) and K_L is the Langmuir equilibrium constant. The values of ΔH^o and ΔS^o were estimated using the following relationships, via plotting ln K_L against $1/T$ [40]:

$$\ln K_L = -\frac{\Delta H^0}{RT} + \frac{\Delta S^0}{R} \quad (2)$$

The calculated thermodynamic values were therefore deduced and reported in Tables 4 and 5. The positive heat of adsorption values suggests again that the interaction of CBY and CBP with studied modified PA materials is endothermic, which is also supported by the increment in adsorption of the corresponding dyes with the increase in temperature and also by the calculated value of sorption energy (B_T) from Temkin equation. Additionally, the negative value of the entropy change (between −32.94 and −5.37) was found to be consistent with the decreased disorder at the solid-solution interface during the adsorption process.

Conclusion

In this paper, we developed an easy and simple method to prepare novel PA-CA-CS materials in order to provide PA fibers with greatly enhanced affinity for reactive dyes. PA samples were modified with CS using CA as cross-linked agent, characterized in terms of FT-IR and TGA-DTA analysis and also compared based on their capacities for the removal of reactive dyes from aqueous suspension. A sort of interaction between CS and PA and CA is proposed based on characterization results. Data gleaned from thermal analysis showed that the prepared materials were found to be more thermally stable than the plain PA due to reticulation phenomenon. Checking their capacities for the adsorption of

reactive dyes, plain PA fibers reveal no affinity for the two studied dyes. However, the removal of these dyes, under the same experimental conditions, are greatly enhanced when the CS molecules where reacted with PA fibers. The registered sorption capacities, at equilibrium, achieved their maximum (21.7 and 35.4 $mg \cdot g^{-1}$, respectively, for CBP and CBY at 22 °C) for a concentration of CS, in bath treatment, of about 0.5 %. The results also exhibited that the adsorption capacities are more important using CA than AA. The rate of adsorption was found to be directly dependent on the dye structure, contact time, initial dye concentration and temperature. The pseudo second-order equation was shown to fit the adsorption phenomenon. The determination of thermodynamic parameters for different experimental conditions allowed the energy, enthalpy and entropy to be calculated. Both kinetic data and calculated constant (E) from Dubinin-Redushkevich equation reveal that the adsorption phenomenon of CBY and CBP is chemical mode. Either effect of temperature, enthalpy change values, or calculated constant (A_T) from Temkin equation suggests the endothermic nature of the process. As these materials are simple to be produced and efficient in target removal, our further works can be extended to look for other supports and also to check the efficiency of these adsorbents for the removal of other toxic pollutants such as pesticides.

Nomenclature

CS : Chitosan
PA : Polyamide
CA: Ciric acid
AA: Acetic acid
q_e : Equilibrium dye concentration on adsorbent, $mg \cdot g^{-1}$
q_t : The amount of dye adsorbed per unit mass of the adsorbent at time, t, $mg \cdot g^{-1}$
C_0 : Initial dye concentration in aqueous solution, $mg \cdot l^{-1}$
C_e : Concentration of the dye at equilibrium, $mg \cdot l^{-1}$
λ_{max}: Maximum wavelength, nm
t : Time, s
$q_{e.1}$: The adsorption capacity of the first order equation, $mg \cdot g^{-1}$
$q_{e.2}$: The adsorption capacity of the second order equation, $mg \cdot g^{-1}$
k_1 : The first order rate constant, min^{-1}
k_2 : The second order rate constant, $l \cdot mg^{-1}$
h : The Elovich constant, $mg \cdot g^{-1} \cdot min^{-1}$
a : Initial sorption rate, $mg \cdot g^{-1} \cdot min^{-1}$
b : Extent of surface coverage, $mg \cdot g^{-1} \cdot min^{-1}$
K_i : The intra-particule diffusion constant, $mg \cdot g^{-1} \cdot min^{1/2}$
C_{eq} : The residual equilibrium concentration, $mg \cdot l^{-1}$
b : Langmuir adsorption constant, $ml \cdot mg^{-1}$
q_m : Theoretical maximum adsorption capacity related to Langmuir, $mg \cdot g^{-1}$
K_F : Freundlich equilibrium constant, $l \cdot g^{-1}$
n : Freundlich constant, indication of the favorability of the studied process
B_T : Temkin constant related to heat of sorption, $J \cdot mol^{-1}$
A_T : Temkin isotherm constant, $l \cdot g^{-1}$
E : Free energy of equation Dubinin-Redushkevich, $kJ \cdot mol^{-1}$
R^2 : Linear regression coefficient
T : The absolute temperature, K
ΔS^o: Entropy change, $J \cdot mol^{-1} \cdot K^{-1}$
ΔH^o: Enthalpy change, $kJ \cdot mol^{-1}$
ΔG^o: Free energy, $kJ \cdot mol^{-1}$

References

1. A. Mittal, D. Kaur, and J. Mittal, *J. Colloid Interf. Sci.,* **326**, 8 (2008).
2. M. Rinaudo, *Prog. Polym. Sci.,* **31**, 603 (2006).
3. R. Jayakumar, M. Prabaharan, R. L. Reis, and J. F. Mano, *Carbohyd. Polym.,* **62**, 142 (2005).
4. N. Sakkayawong, P. Thiravetyan, and W. Nakbanpote, *J. Colloid Interf. Sci.,* **286**, 36 (2005).
5. G. Annadurai, L. Y. Ling, and J. F. Lee, *J. Hazard. Mater.,* **152**, 337 (2008).
6. W. S. Wan Ngah, L. C. Teong, and M. A. K. M. Hanafiah, *Carbohyd. Polym*., **83**, 1446 (2011).
7. M. Jabli, M. H. V. Baouab, S. N. Zydowicz, and B. Ben Hassine, *J. Appl. Polym. Sci.*, **123**, 3412 (2011).
8. M. Jabli, R. Touati, Y. Kacem, and B. Ben Hassine, *J. Text. Inst.*, **103**, 434 (2012).
9. C.-M. Shih, Y.-T. Shieh, and Y.-K. Twu, *Carbohydr. Polym*., **78**, 169 (2009).
10. F. Lidija, R. Tijana, and T. Tina, *J. Eng. Fibers Fabr.*, **7**, 50 (2012).
11. Y. C. Nho and K. R. Park, *J. Appl. Polym. Sci.*, **85**, 1787 (2002).
12. W. S. Wan Ngah, K. Kamari, and Y. J. Koay, *Int. J. Biol. Macromol.*, **34**, 155 (2004).
13. M. Zeng, H. Xiao, X. Zhang, X. Sun, C. Qi, and B. Wang, *J. Macromol. Sci., Part B: Phys*., **50**, 1413 (2011).
14. J.-T. Yeh, C.-L. Chen, K. S. Huang, Y. H. Nien, J. L. Chen, and P. Z. Huang, *J. Appl. Polym. Sci.*, **101**, 885 (2006).
15. B. G. Min and C. W. Kim, *J. Appl. Polym. Sci.*, **84**, 2505 (2002).
16. Y. Ma, T. Zhou, and C. S. Zhao, *Carbohyd. Res.*, **343**, 230 (2008).
17. C. Makhlouf, M. H. V. Baouab, and S. Roudesli, *Adsorpt. Sci. Technol.*, **26**, 433 (2008).
18. H.-J. Tseng, S.-H. Hsu, M.-W. Wu, T.-H. Hsueh, and P.-C. Tu, *Fiber. Polym.*, **10**, 53 (2009).
19. M. Jabli, M. H. V. Baouab, S. Roudesli, and A. Bartegi, *J. Eng. Fibers Fabr.*, **6**, 1 (2011).
20. M. Jabli, F. Aloui, and B. Ben Hassine, *J. Eng. Fibers Fabr.*, **8**, 1 (2013).
21. S. H. Hsieh, Z. K. Huang, Z. Z. Huang, and Z. S. Tseng, *J. Appl. Polym. Sci.*, **94**, 1999 (2004).

22. Y. Li, Z. M. Huang, and Y. D. Lu, *Eur. Polym. J.,* **42**, 1696 (2006).
23. N. Prakash, P. N. Sudha, and N. G. Renganathan, *Environ. Sci. Pollut. Res.,* **19**, 2930 (2012).
24. J. Junkasem, R. Rujiravanit, and R. P. Supaphol, *Nanotechnology*, **17**, 4519 (2006).
25. T. Wang, M. Turhan, and S. Gunasekaran, *Polym. Int.*, **53**, 911 (2004).
26. Y. S. Ho and G. McKay, *Water Res.*, **33**, 578 (1999).
27. Y. S. Ho and G. McKay, *Process Biochem.*, **34**, 451 (1999).
28. A. Ornek, M. Ozacar, and A. Sengil, *Biochem. Eng. J.*, **37**, 192 (2007).
29. G. Grini, H. N. Peindy, F. Gimbert, and C. Robert, *Sep. Purif. Technol.*, **53**, 97 (2007).
30. K. K. Panday and V. N. Prasad, *Environ. Technol. Lett.*, **50**, 547 (1986).
31 I. Langmuir, *J. Am. Chem. Soc.,* **40**, 1361 (1918).
32. H. Freundlich, "Colloid and Capillary Chemistry", p.523, Mateun & Co., Ltd., London, 1926.
33. A. U. Itodo and H. U. Itodo, *Life Sci. J.*, **7**, 31 (2010).
34. M. Horsfall and A. I. A. A. Abia, *Bull. Korean Chem. Soc.*, **25**, 969 (2004).
35. R. E. Treybal, "Mass Transfer Operations", 3rd Ed., McGraw Hill, NewYork, 1980.
36. C. Li, H. Chen, and Z. Li, *Proc. Biochem*., **39**, 541 (2004).
37. M. T. Ikhlass, Thèse de doctorat en chimie, Université Paris-Est Créteil ICMPE, 2012.
38. S. Rengaraja, J.-W. Yeon, Y. Kim, Y. Jung, Y.-K. Ha, and W.-H. Kim, *J. Hazard. Mater.*, **143**, 469 (2007).
39. Y. C. Sharma, G. Prasad, and D. C. Rupainwar, *Int. J. Environ. Stud.*, **37**, 183 (1991).
40. A. K. Jain, V. K. Gupta, A. Bhatnagar, and Suhas, *J. Hazard. Mater.*, **101**, 31 (2003).